Joining of High-Nitrogen Stainless Steel by Capacitor Discharge Welding

The rapid cooling rate of the process is an advantage in retaining the strength properties of high-nitrogen alloys

BY J. W. SIMMONS AND R. D. WILSON

ABSTRACT. The effectiveness of nitrogen as an interstitial strengthening agent has led to the development of a new class of austenitic stainless steels — high-nitrogen alloys defined by their nitrogen contents (generally >0.4 wt-% N). Unlike most alloying elements, nitrogen has a very limited solubility in liquid iron-based alloys at atmospheric pressure. Therefore, high-nitrogen stainless steels are produced by high-pressure melting. Joining of high-nitrogen stainless steels presents unique challenges since the nonequilibrium nature of the material results in loss of nitrogen from the fusion and partially melted zones during welding procedures typically utilized for stainless steels, such as gas tungsten arc welding (GTAW). Loss of nitrogen from the molten base metal can result in severe weld porosity and reduced solid-solution strengthening. In this study, rapid solidification joining of a high-nitrogen stainless steel by capacitor discharge welding resulted in complete retention of the nonequilibrium level of nitrogen in the material, which is responsible for the alloys's high strength. Joining of the high-nitrogen material using optimized welding parameters produced virtually porosity-free welds with joint efficiencies greater than 95% and no heat-affected zone. Optimization of welding parameters was aided by the use of a computer-based data collection system, which allows for a systematic analysis of the effect of welding parameters on weld properties.

J. W. SIMMONS and R. D. WILSON are with U.S. Bureau of Mines, Albany, Ore.

Introduction

High-nitrogen stainless steels are becoming an increasingly important new class of engineering materials and have been the subject of four international conferences.[1] Unlike most alloying elements, nitrogen has a very limited solubility in liquid iron-based alloys. The solubility of nitrogen in pure liquid iron at atmospheric pressure is only 0.045 wt-% (Refs. 1, 2). Any excess nitrogen in the liquid metal will simply evolve from the melt as a gas. Fortunately, nitrogen solubility in liquid iron-based alloys can be increased through alloy additions like Cr and Mn and by increasing the gas pressure above the melt. A stainless steel can be considered to be a high-nitrogen alloy if it contains more nitrogen than can be retained in the material by processing at atmospheric pressure. For most alloys, this limit is about 0.4 wt-% nitrogen.

Nitrogen alloying has several beneficial effects in austenitic stainless steels: 1) nitrogen is a more effective solid-solution strengthener than carbon and also enhances grain size (Hall-Petch) strengthening (Refs. 3, 4); 2) nitrogen is a strong austenite stabilizer, thereby reducing the amount of nickel required for stabilization and reduces the tendency to form ferrite or deformation-induced martensite (Ref. 5); 3) nitrogen has greater solid-solubility than carbon, thus decreasing the tendency for precipitation at a given level of strengthening (Ref. 6). Yield and tensile strengths of high-nitrogen (>0.4 wt-% N) materials exceed those of the traditional AISI 200 and 300 series stainless steels by 200–300% in the annealed condition, without sacrificing toughness (Ref. 7). Cold deformation can produce further increases in strength resulting in materials with yield strengths above 2 GPa (Ref. 8). Alloying to the levels of nitrogen required to produce these enhanced mechanical properties requires material production by melting under high N_2 gas overpressures, since the solubility of N in liquid iron-based alloys is very limited at atmospheric pressure. Recent advances in processing technologies have resulted in the commercial production of high-nitrogen alloys containing over 1 wt-% N (Ref. 9).

Joining of high-nitrogen stainless steels presents unique challenges since the nonequilibrium nature of the material results in loss of nitrogen from the fusion and partially melted zones during welding procedures typically utilized for stainless steels, such as gas tungsten arc

KEY WORDS

High-N Stainless Steel
Capacitor Discharge
Porosity-Free
Nitrogen Solubility
Welding Stainless
Welding Parameters
Heat-Affected Zone
Microstructure

1. High Nitrogen Steels (HNS 88), Lille, France; HNS 90, Aachen, Germany; (HNS 93) Kiev, Ukraine; HNS 95, Kyoto, Japan.

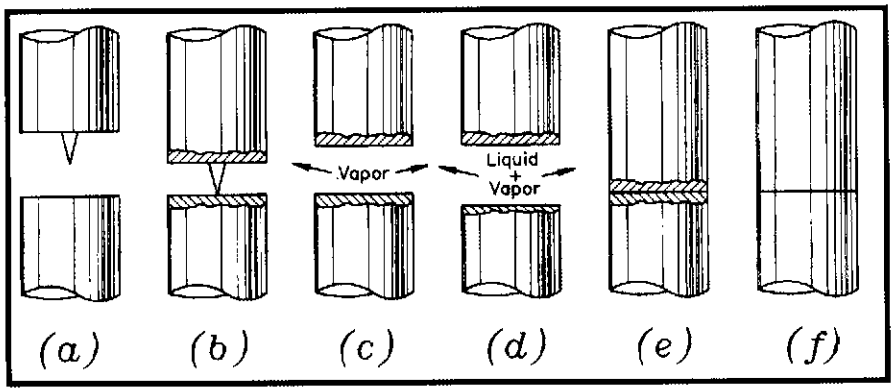

Fig. 1 — Schematic of the CDW process: A — cathode positioned above anode; B — arc ignition at the welding tip; C — plasma expulsion; D — ejection and condensation of plasma into small metal particles; E, F — CD joint after electrode contact.

welding (GTAW) (Ref. 10). Loss of nitrogen from the molten base metal can result in severe weld porosity and reduced solid-solution strengthening. Rapid solidification joining by capacitor discharge welding (CDW) offers a unique opportunity to join these materials without nitrogen loss or weld porosity, thus producing joints with strengths approaching that of the base material. The rapid solidification nature of the CDW process enables nonequilibrium microstructures to be maintained in the fusion zone with the production of a minimal, or nonexistent, heat-affected zone (HAZ). In this study, cylinders (6.35-mm diameter) of a high-nitrogen stainless steel were welded using CDW. Mechanical and microstructural evaluation of the CD welds was conducted and the results compared to autogenous gas tungsten arc welds (GTAW) made with the same material. This study illustrates the advantages of the CDW process in maintaining and/or producing nonequilibrium structures and its applicability to joining high-nitrogen steels.

The Capacitor Discharge Welding Process

Capacitor discharge welding is a rapid solidification joining process which produces cooling rates as fast as 10^5–10^6 K/s (Refs. 11–13). The CDW unit at the U.S. Bureau of Mines Albany Research Center consists of a capacitor bank, a power supply for charging the capacitors, and the electrodes to be welded. Data acquisition and automated control is accomplished through connection to a PC-based computer via an analog-to-digital data converter. Analysis of CDW using high-speed photography has shown that the entire welding process takes from 1 to 3 ms (Ref. 14).

The CDW process is illustrated schematically in Fig. 1. Prior to arc initiation, the capacitor bank is fully charged and the resistance of the circuit is infinite. The tip of the cathode striking the anode causes discharging of the capacitor bank, initiating the arc (Fig. 1B). The arc quickly spreads across the electrode face (Fig. 1C). As the plasma moves away from the joint, the superheated vapor cools and condenses into spherical metal particles (Fig. 1D). As the electrodes make contact (Fig. 1E), the resistance and voltage of the circuit decrease and approach zero — Fig. 2. The layer of liquid metal at the electrode interface then solidifies to form the joint. The fusion zone in CD welds is generally less than 100 μm thick, and the heat affected zone (HAZ) is in most cases, undetectable, thereby preserving the metallurgical properties of the base metal (Ref. 14).

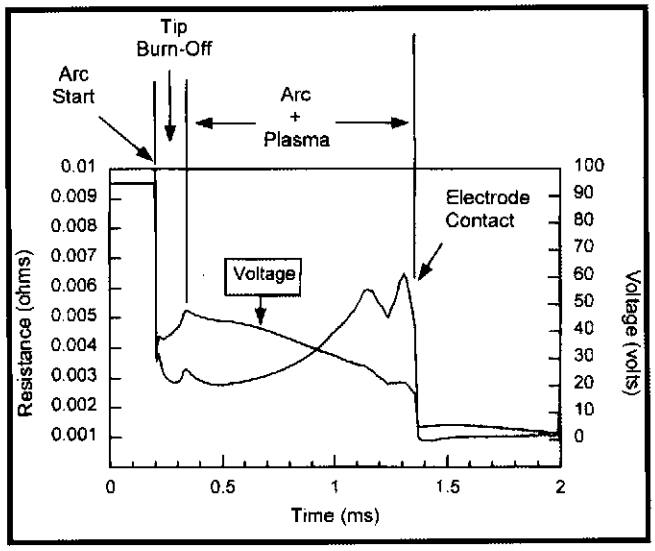

Fig. 2 — Electrical resistance and voltage across the joint as a function of discharge time. The voltage and resistance approach zero as the electrodes make contact.

Data, typical of that which can be collected during the welding process (*e.g.*, voltage, current, and resistance vs. time plots) are shown in Fig. 2. Acquisition and analysis of such data has led not only to a greater understanding of the welding process itself, but enables rapid adjustments of the welding parameters, resulting in increased joint efficiency; all but eliminating the trial and error approach to optimizing welding parameters. The rapid solidification nature of the CDW process enables nonequilibrium microstructures to be retained. CDW can be automated to accommodate high production rates and since welds do not penetrate through the base metal, parts can be welded onto sealed containers. The process requires that a precision arc ignition tip be machined on one of the electrodes to initiate the welding process. Dissimilar metals, composites, or ceramics can be welded if they are electrically conductive.

The important factors controlling the CDW process are welding tip length (L), capacitance (c), voltage (v), and electrode separation (*i.e.*, drop height (H)). The total energy input (E) is defined by Equation 1. The tip length essentially controls the welding time (T_w, the time between when the cathode tip strikes the anode and when the two parts actually come in contact), defined by Equation 2, where g is the acceleration of gravity. If the welding time is considerably longer than 2RC (two times the time-constant, the product of the resistance and capacitance, with units of time), the molten metal on the electrode surfaces can solidify before joint closure, causing presolidification and reducing joint strength. Too short of a welding time results in poor electrode fusion because the capacitors cannot completely discharge before electrode contact. Insufficient energy input can also lead to weld porosity caused by extinguishment of the arc before it travels across the entire electrode surface. This is referred to as incomplete fusion.

$$E = \frac{1}{2}cv^2 \qquad (1)$$

$$T_w = \frac{L}{\sqrt{2gH}} \qquad (2)$$

Experimental Procedures

The composition of the high-nitrogen stainless steel employed in this study is listed in Table 1. The material, which contained 0.69 wt-% nitrogen, was produced by pressurized electroslag remelting (PESR) as an 8-ton ingot in a full-scale commercial facility. The details of the PESR method for producing high-nitrogen steels have been described elsewhere (Ref. 9). To ensure that all of the nitrogen present in the material was dissolved interstitially, the material was solution annealed at 1150°C (2102°F) for 2 h, followed by water quenching. After this annealing treatment, the grain size of the material was nominally 70μm. Each CD weld was produced using a pair of cylindrical electrodes (anode and cathode) as previously illustrated in Fig. 1. The electrodes were 6.35 mm (1/4 in.) in diameter and approximately 35 mm (1.4 in.) in length. An ignition tip (0.635 mm long) was machined onto the center of each cathode. In preparing the tip, the face of the cylinder was machined with a 4-deg bevel with respect to the cylinder axis. The bevel reduces weld porosity by ensuring that metal vapor and gas are not trapped in the molten weld metal. The range of parameters used during the CDW experiment are listed in Table 2. Total energy inputs (calculated using Equation 1) between 280 and 850 J were generated by varying the voltage and capacitance. Tensile testing and metallographic analyses were performed on the welds as a function of energy input. Microprobe analysis of the nitrogen concentration across the weld region in selected CDW specimens was performed on metallographically prepared sections. Multiple microprobe analyses within the high-nitrogen steel matrix indicated that the standard deviation in the microprobe measurements was 0.05 wt-% nitrogen.

For purposes of microstructural comparison to the CD welds, autogenous welds were made on plates of the same high-nitrogen steel using the GTAW process. Two heat inputs, 335 and 402 kJ/m (8.5 and 10.2 kJ/in.) were used. The fusion zone of each weld was subsequently evaluated for retained nitrogen and ferrite content. The ferrite content in the fusion zone was estimated using a ferrite gauge; the base metal was fully austenitic. Comparison of the nitrogen concentration in the CD- and GTA-welded samples was done by removing the weld metal and performing a bulk nitrogen analysis using a commercial inert gas fusion-type analysis unit.

Results and Analysis

The high-nitrogen material used in this study contained much more nitrogen than can be retained in the liquid metal at atmospheric pressure. This is illustrated in the diagram of Fig. 3, which shows the nitrogen solubility in this alloy as a function of pressure. Generally, at nitrogen concentrations below about 1 wt-%, the solubility of nitrogen in liquid iron-based alloys follows Sievert's Law (the nitrogen solubility is proportional to the square root of the gas pressure). However, as nitrogen concentrations increase within the melt (*i.e.*, with increasing pressure), nitrogen-nitrogen interactions within the molten metal cause deviations from Sievert's Law (*i.e.*, pressure increases are less effective than predicted). For the alloy used in this study, a nitrogen overpressure of about 10 atmospheres is needed to retain 0.69 wt-% nitrogen in the molten material at 1600°C (2912°F). Since the nitrogen solubility in the material at atmospheric pressure is about 0.31 wt-%, melting the material at pressures below 10 atmospheres results in loss of nitrogen.

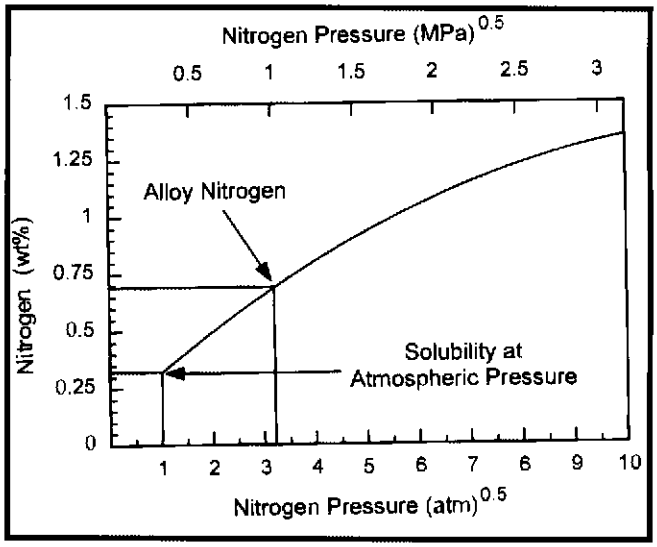

Fig. 3 — Effect of pressure on nitrogen solubility in liquid Fe-19Cr-5Mn-5Ni-3Mo alloy at 1600°C.

Lundin and Qiao (Ref. 10) have already shown that autogenous GTA welding of high-nitrogen stainless steel results in the formation of a "porosity belt" in the fusion and partially melted regions of the weld. The formation of ferrite in the fusion zone of the autogenous GTA weld was attributed to loss of nitrogen from the molten metal during the welding process. The formation of significant porosity in a critical region of a fusion weld, such as in the fusion and partially melted zones, has obvious detrimental effects on material performance. The formation of ferrite in the fusion zone could also be detrimental to material performance in certain applications where the nonmagnetic properties of the alloy need to be maintained. Loss of nitrogen from the fusion zone reduces the overall joint integrity since interstitial strengthening by nitrogen is the primary strengthening mechanism for the alloy.

In this study, capacitor discharge welds made using heat inputs of less than 700 J typically had tensile strengths that were less than 50% of the base metal strength. Low heat inputs (*i.e.*, less than 700 J) were not sufficient to sustain arc travel all the way across the electrode surfaces and therefore resulted in only partial bonding of the two electrodes. These lower heat inputs resulted in less molten metal on the electrode surfaces, which resulted in only partial melting of the electrode surfaces. Also, the surfaces that had melted tended to solidify prior to the parts coming together. These phenomena are referred to as presolidification. An optical micrograph taken from a weld with significant pre-solidification is shown in Fig. 4. The total thickness of the weld joint shown in Fig. 4 was only about 25 μm. In this case, the presolidification was caused by using too low of an energy

Table 1 — Composition of High-Nitrogen Austenitic Stainless Steel (wt-%)

Fe	Cr	Mn	Ni	Mo	Si	C	N
Bal.	19.3	5.2	5.2	2.9	0.86	0.024	0.69

Table 2 — Capacitor Discharge Welding Process Parameters for High-Nitrogen Austenitic Stainless Steel

Capacitance	78,000–153,600 μF
Voltage	70.5–105.2 V
Energy input	280–850 J
Drop height	38 mm (1.5 in.)
Electrode geometry	6.35 mm (0.25 in.) Diameter cylinders
Tip length	0.635 mm (0.025 in.)

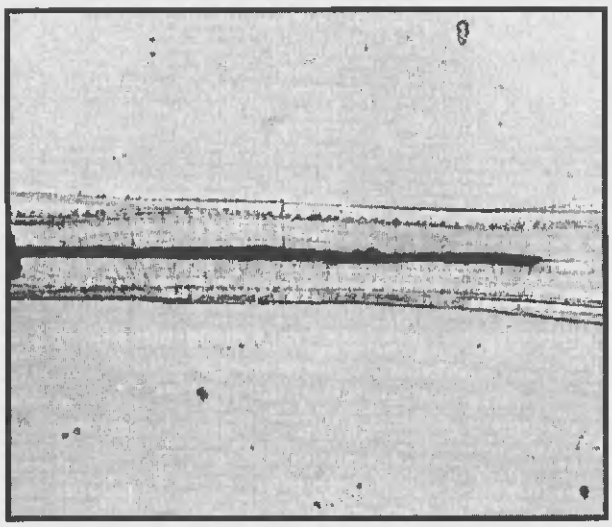

Fig. 4 — Optical micrograph of cross-sectioned CD weld showing presolidification caused by insufficient heat input (650 J). Electrolytically etched using an aqueous solution containing 10% oxalic acid.

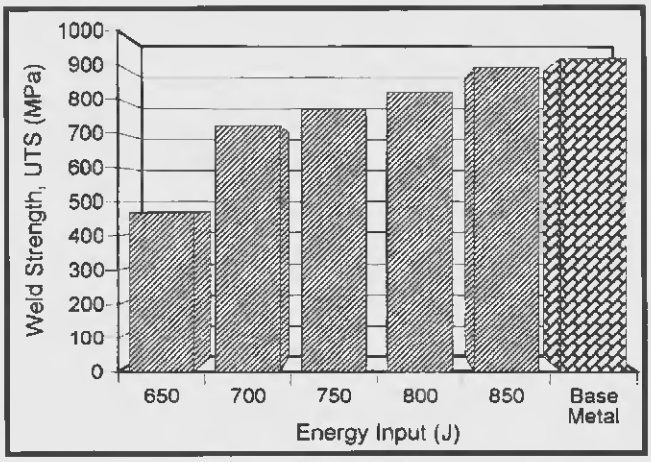

Fig. 5 — Ultimate tensile strengths achieved for high-nitrogen stainless steel welds produced by capacitor discharge welding.

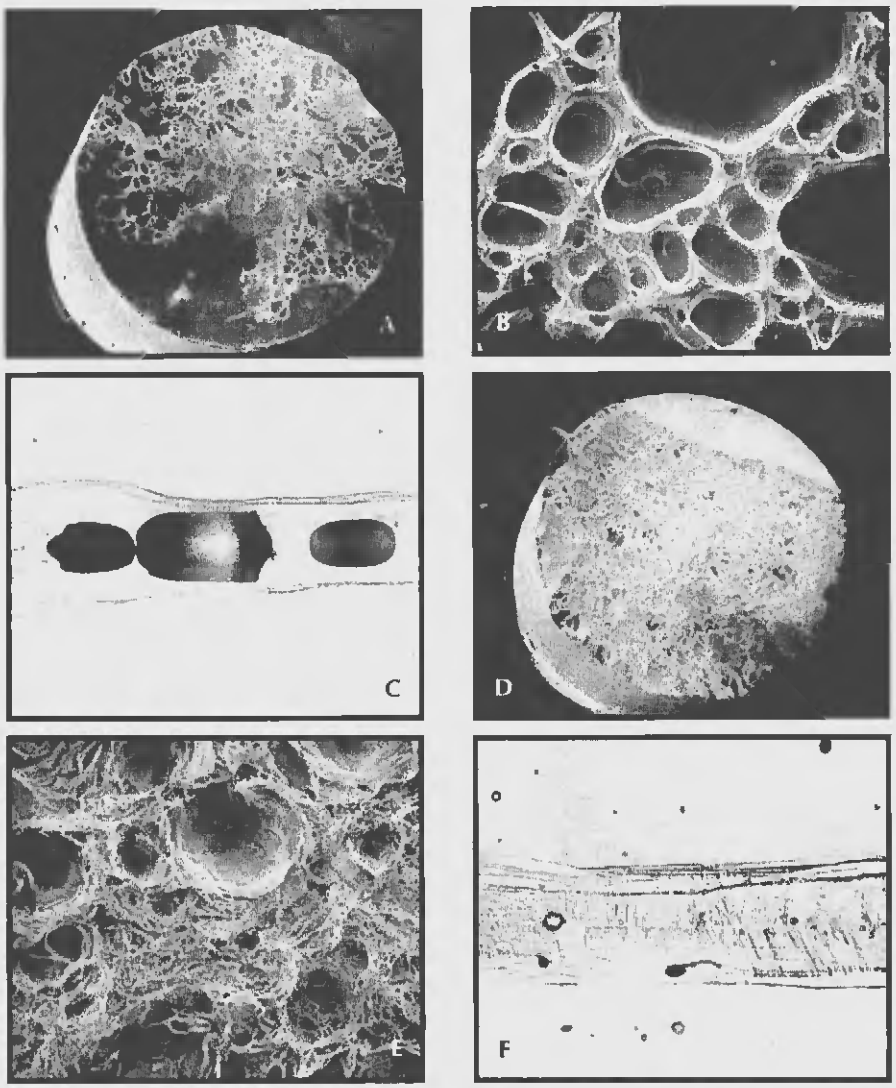

Fig. 6 — Scanning electron fractographs of tensile specimens capacitor discharge welded at heat inputs of: A, B — 650 J; D, E — 850 J. Optical micrographs of cross-sectioned welds made using heat inputs of: C — 650 J; D — 850 J (samples electrolytically etched using an aqueous solution containing 10% oxalic acid).

input (650 J). The low heat input, in conjunction with the welding time, allowed complete solidification of the molten metal in some areas of the weld prior to contact of the two electrode surfaces.

Tensile strengths achieved using heat inputs of 650–850 J are shown in Fig. 5. For these welds, a constant capacitance of 153,600 μf was used and the energy input (Equation 1) was changed by adjusting the voltage. The weld strength increased with increasing energy input up to 850 J, where joint efficiencies of over 95% were obtained. Increasing the energy input beyond 850 J resulted in excessive expulsion of molten metal from the fusion zone, creating "flash" on the electrodes, outside of the weld joint. The increase in joint strength with increasing energy input was simply due to the increased weld area (decrease in unfused regions within the fusion zone) associated with higher heat inputs. The total heat input into the CD weld joint must be high enough to 1) cause complete melting of the electrode tip, 2) sustain arc travel and cause melting across the entire electrode surfaces, and 3) melt enough material to ensure that the thickness of the molten layer on each electrode is thick enough so that complete solidification does not occur prior to the parts coming together.

Scanning electron fractographs and optical micrographs (Fig. 6) illustrate the characteristics of samples welded with heat inputs of 650 and 850 J. Samples welded at the lower heat inputs (*e.g.*, 650 J) suffered from two primary, but related, problems. First, a lack of sufficient heat input resulted in incomplete melting of the electrode tip on the cathode, which

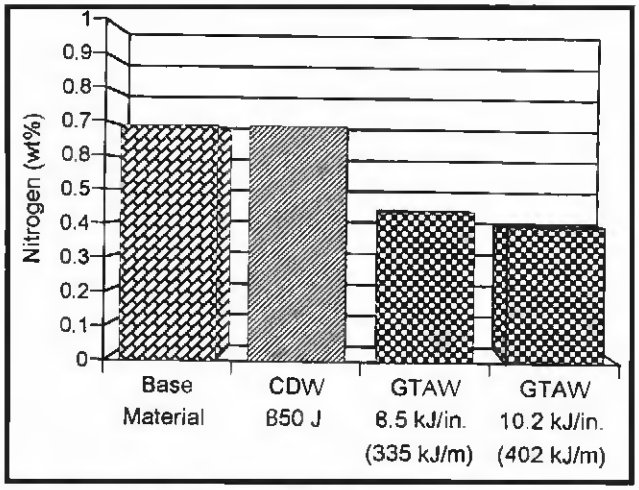

Fig. 7 — Measured nitrogen concentrations in autogenous welds and base alloy.

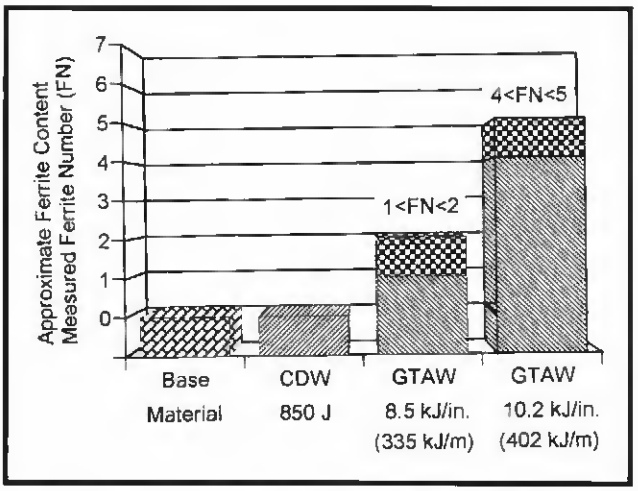

Fig. 8 — Comparison of ferrite contents in autogenous welds and base alloy.

tended to keep the parts from completely coming together. Secondly, only a portion of the electrode surfaces were melted, thereby limiting the weld area. Due to only partial fusion of the two surfaces in low-heat-input welds, low joint efficiencies were obtained. These features of the low-energy-input welds can be seen in the SEM fractographs of Fig. 6A and B. The smooth surface features of Fig. 6A correlate to the electrode surfaces that were not fused at all. These areas of the electrode surface were either not melted at all or contained such a thin layer of liquid metal that presolidification prevented any fusion from occurring in those areas. Although the fracture mechanism itself was ductile, the areas between the fracture ridges shown in Fig. 6B are not dimples caused by microvoid coalescence, but actual voids in the weld. Welding with a heat input of 850 J resulted in complete tip melt-off and melting of the electrode surfaces, and high joint efficiencies. The characteristics of the high-energy welds are illustrated by the micrographs shown in Fig. 6D, E and F. The ductile nature of the high-energy welds, which were virtually void-free and had a dimpled-rupture fracture appearance, is shown in the SEM fractograph of Fig. 6E.

Due to the rapid solidification nature of the CDW process, all of the nitrogen present in the material, although melted under nonequilibrium conditions, was retained in the weld metal. This is illustrated in Fig. 7, which shows the bulk nitrogen concentrations of the CD and GTA welds measured by inert carrier gas fusion. The bead-on-plate welds made with the GTA process resulted in nitrogen levels that were significantly below the level of the base material, but were slightly above the equilibrium nitrogen concentration of the material at atmospheric pressure. Microprobe analyses of metallographically prepared cross-sections of several CD welds correlated with the bulk nitrogen analysis shown in Fig. 7. Therefore, in CD welds, the metal in the fusion zone contained the same level of nitrogen as the base metal. The retention of nitrogen in the weld makes it possible to achieve high joint efficiencies since every 0.1 wt-% of nitrogen lost results in about a 60 MPa decrease in the tensile strength of the material. It should be remembered, however, that weld porosity or incomplete weld fusion, such as that observed in welds with low heat inputs, is more detrimental to weld strength than loss of nitrogen. The loss of nitrogen from the GTA welds resulted in ferrite formation since this alloy relies on its high nitrogen concentration for stabilization of the austenite. In contrast, the CD welds did not contain any ferrite — Fig. 8.

To illustrate the fact that CDW results in the production of a HAZ-free weldment, CD welds were produced on the same high-nitrogen steel after aging at 950°C (1742°F) for 3 h. This aging treatment resulted in the grain boundary, cellular, and transgranular precipitation of nitrides (Cr_2N). The cellular precipitation products comprised about 40 vol-% of the material. The morphology of the cellular precipitate is essentially identical to pearlite formed in carbon steels. The resulting weld cross-section of the aged material is an excellent illustration of the weld characteristics produced by the CDW process (see optical micrograph of Fig. 9). Weld solidification nucleates and grows epitaxially from the molten-metal/solid-metal interface of each electrode. Solidification of the weld metal is completed when the two solidifying interfaces impinge on one another at the centerline between the two electrodes. The fine cells, characteristic of the cellular solidification of the weld metal, can be seen in the optical micrograph of Fig. 9. The total

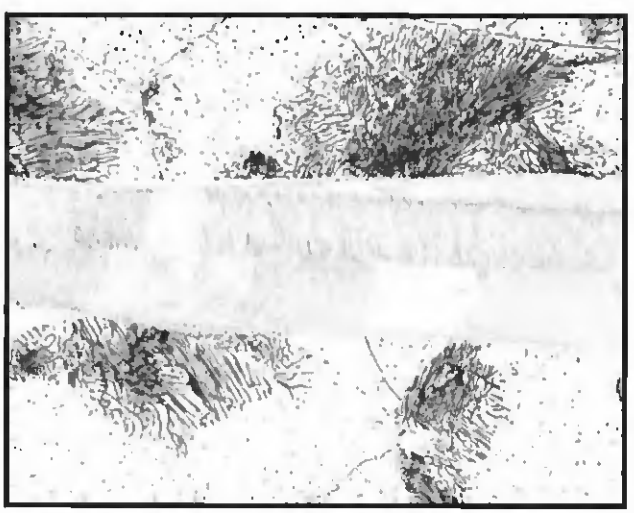

Fig. 9 — Optical micrograph, taken from specimen aged at 950°C for 3 h prior to CD welding, illustrating the total lack of any heat-affected zone produced by the CDW process. Electrolytically etched using an aqueous solution containing 10% oxalic acid.

lack of any HAZ can also be seen in the micrograph by examining the weld/base metal interface. The nitrides present in the aged material essentially melted off at the interface and absolutely no change in the microstructure occurred outside of the fusion zone.

Conclusions

Rapid solidification joining of a high-nitrogen stainless steel by CDW resulted in complete retention of the nonequilibrium level of nitrogen in the material, which is responsible for the alloys' high strength. This study showed that joining of high-nitrogen materials using optimized CDW parameters produces virtually porosity-free welds with joint efficiencies greater than 95%. Also, no detectable HAZ was present in the CD welds. Conversely, GTAW of the material resulted in significant losses of nitrogen, which, based solely un the luss of interstitial solid-solution strengthening due to nitrogen, would reduce obtainable joint efficiencies to less than 80%. Optimization of welding parameters was aided by the use of a computer-based data collection system, which allows for a more systematic analysis of the effect of welding parameters on weld properties.

References

1. Pehlke, R. D., and Elliott, J. F. 1960. Solubility of nitrogen in liquid iron alloys. 1. *Thermodynamics, Trans. AIME* 218: 1088–1101.

2. Satir-Kolorz, A. H., and Feichtinger, H. K. 1991. *Z. Metallkunde* 82 (9): 689–697.

3. Byrnes, M. L. G., Grujicic, M., and Owen, W. S. 1987. Nitrogen strengthening of a stable austenitic stainless steel. *Acta Metall.* 35(7): 1853–1862.

4. Werner, E. 1988. Solid solution and grain size hardening of nitrogen-alloyed austenitic steels. *Mat. Sci. and Engr. A* 101: 93–98.

5. Reed, R. P. 1989. Nitrogen in austenitic stainless steels. *JOM* (March): 16-21.

6. Kikuchi, M., Kajihara, M., and Frisk, K. 1989. Solubility of nitrogen in austenitic stainless steels. *Proceedings of the International Conference on High Nitrogen Steels, HNS 88, Lille, France.* eds. J. Foct and A. Hendry, pp. 63–74. The Institute of Metals.

7. Simmons, J. W. 1994. High-nitrogen alloying of stainless steels. *Microstructural Science Vol. 21.* pp. 33–49, ASM International, Materials Park, Ohio.

8. Speidel, M. O. 1989. Properties and Applications of High Nitrogen Steels. *Proceedings of the International Conference on High Nitrogen Steels, HNS 88, Lille, France.* eds. by J. Foct and A. Hendry, pp. 92–96. The Institute of Metals.

9. Stein, G., Menzel, J., and Dorr, H. 1989. Industrial Manufacture of Massively Nitrogen-Alloyed Steels. *Proceedings of the International Conference on High Nitrogen Steels, HNS 88, Lille, France.* eds. J. Foct and A. Hendry, pp. 32–38. The Institute of Metals.

10. Lundin, C.D., and Qiao, C.Y.P. 1992. Fusion zone and heat-affected zone microstructure in high-nitrogen stainless steel. *International Trends in Welding Science and Technology, Proceedings of the 3rd International Conference on Trends in Welding Research, Gatlingburg, TN.* eds. S. A. David and J. M. Vitek. pp. 247–251. ASM International, Materials Park, Ohio.

11. Wilson, R. D., Woodyard J. R., and Devletian, J. H. 1993. Capacitor discharge welding: analysis through ultrahigh-speed photography. *Welding Journal* 72 (3): 101-s to 106-s.

12. Venkataraman, S., and Devletian, J. H. 1988. Rapid solidification of stainless steel by capacitor discharge welding. *Welding Journal* 67(6): 111-s to 118-s.

13. Einerson, C. J., Clark, D. E., and Devletian, J. H. 1987. *Proc. of the 1987 ASME/JSME Thermal Engineering Joint Conf., Vol. 3.* eds. P. J. Marto and I. Tanasawa, p. 217. ASME.

14. Wilson, R. D., Hawk, J. A., and Devletian, J. H. 1993. Capacitor discharge weld modeling using ultra high speed photography. *Mat. Res. Soc. Symp. Proc.*, Vol. 314. pp. 151–162. Materials Research Society.